Proceedings World Geothermal Congress 2015
Melbourne, Australia, 19-25 April 2015

TherMAP – Assessing Subsurface Temperatures in Australia from a Geothermal Systems Perspective

Marcus W. Haynes, Anthony R. Budd, Ed J. Gerner, Chris Harris-Pascal, and Alison L. Kirkby

GPO Box 378, Canberra, ACT, 2601, Australia

Marcus.Haynes@ga.gov.au

Keywords: Australia, Thermal modelling, Underworld, National Computational Infrastructure, uncertainty analysis, stochastic methods

ABSTRACT

Understanding the distribution of subsurface temperatures is an important early step in a geothermal exploration process. With the exception of a few areas of hot springs, there are no surface manifestations of anomalous temperature at depth in Australia. The Australian continent has no active magmatism, the deep heat flow regime is conductive, and thick layers of insulating sediments are necessary to obtain elevated temperatures at depths suitable for electricity generation or industrial use. The distribution of direct temperature measurements and surface heat flow determinations is described in Gerner and Holgate (2010). The majority of these measurements were made by the petroleum industry and, while there are over 5000 wells, they are heterogeneously distributed, resulting in unconstrained temperature uncertainties over many parts of the continent. An alternative approach is needed to provide indications of temperature at depth in uncharacterised areas, so that the whole of Australia can be evaluated for geothermal prospectivity. A new approach for developing a 3D temperature map of the Australian continent is being developed that combines available proxy data using high-performance computing and large continental-scale datasets. The Thermal Map from Assessed Proxies (TherMAP) is a new 3D modelling approach that brings together up-to-date national-scale datasets collected by Geoscience Australia and others, including OzTemp, OZ SEEBASE^{TM}, OZCHEM, surface temperature, Australian Geological Provinces, Moho depth, thermal conductivity of sedimentary basins and the National Gravity Map of Australia. Bringing together such a range of datasets provides a geoscientific basis by which to estimate temperature in regions where direct observations are not available. Furthermore, the performance of computing facilities, such as the Australian National University's (ANU) National Computational Infrastructure (NCI), is enabling insights into the nature of Australia's geothermal resources that had not been previously available. This includes developing an understanding of the errors involved in such a mapping study through the quantification of uncertainties. At this stage the reported uncertainties around thermal anomalies remain high, but still provide a basis by which to assess temperature estimates at different locations. Encouragingly, TherMAP has been able to reproduce many observed temperature features without using direct bore-hole temperature observations as an input into the modelling process. Furthermore, a number of areas have been identified, due to the difference in estimated temperature distributions from previous methods, which may warrant further study.

1. INTRODUCTION

Geothermal systems are fundamentally defined by two basic parameters; heat flow and fluid flow. Understanding the distribution of subsurface temperatures is, therefore, generally the first step in a geothermal exploration process. However, exploration for areas of anomalous temperature in conduction-dominated geological settings, such as Australia, is complicated by the lack of obvious magmatic activity or surface manifestations, and the depths of the resources. In these regions, different exploration models are needed to identify areas that may have prospective geothermal resources.

The release of the Hot Dry Rock Feasibility Study (Somerville *et al.*, 1994) was a key event that lead to the establishment of the Australian geothermal energy industry. That report compiled the bottom-hole temperature measurements from over 4000 (mainly petroleum) drill holes across the continent. The temperature gradients of these observations were then extrapolated to 5 km depth, and interpolated to create a map of estimated subsurface temperatures.

Since 1994, the Australian bottom-hole temperature database has been updated and developed, with releases under the titles 'Austherm' (Chopra and Holgate, 2005), and later 'OzTemp' (Gerner *et al.*, 2010). The conductive nature of Australia's thermal regime (characteristically of stable continental blocks; Sass and Lachenbruch, 1979) saw the introduction of a simple two-layer model (crystalline basement overlain by sediments) for temperature extrapolation in the OzTemp dataset (Holgate and Gerner, 2010). This was achieved through consideration of the physical processes involved in heat transport and, specifically, through the application of the heat flow equation (Equation 1; Beardsmore and Cull, 2001):

$$Q = -\lambda\left(\frac{\Delta T}{\Delta z}\right) \quad (1)$$

The heat flow equation allows the difference in temperature (ΔT) to be predicted between any two points, as long as information is known on the thermal conductivity of the medium(s) (λ), the distance between the two points (Δz), and the heat flowing between them (Q). This was the first development towards a systems approach for Australian continental temperature estimation and allowed the observed thermal gradients to be modified using assumptions regarding the nature and thermal properties of the geology above or below the observation depth. While this substantially improved the basis for the 1D depth extrapolations, the sparse and uneven distribution of bottom-hole temperature measurements meant that the temperature estimates for large areas were still controlled by the interpolation between distant points.

One of the first major reports to use the heat flow equation to assess geothermal resources at a large-scale was for the United States of America (MIT, 2006). Unlike OzTemp, the MIT study moved away from reliance on disparate data points and began to apply the heat flow equation in modelling 1D temperature profiles along a regularised grid. In adopting this approach, the MIT report may have been the first to recognise that geoscientific information is available that can be used to populate the heat flow equation in areas outside of direct temperature observations. In their report, some broad assumptions about continental heat flow and thermal conductivity values were incorporated into a simple structural model.

Beardsmore *et al.* (2010) later built on the methods of the MIT report to propose a new protocol for the estimation and mapping of enhanced geothermal systems potential, particularly at the regional scale. Along with a regularly-gridded two-layer model, the protocol created a standardised framework by which to assign thermal rock properties for different regions where various levels of geological information may be available. This is important, as it formalises a basis by which to compare the results of studies that have been conducted on different areas. However, an appreciation of the uncertainties of estimates remained elusive.

In recent times, the application of the heat flow equation has also included more detailed 3D models on local-to-regional scales (e.g. Danis and O'Neill, 2009; Cooper and Beardsmore, 2010; Felix *et al.*, 2010). The shift towards 3D modelling, employing the heat flow equation, has also enabled bottom-hole temperature measurements to be used to refine our understanding of the thermal rock properties of different regions, and for an appreciation of uncertainties in the subsurface estimates to be developed (Meixner *et al.*, 2012). However, until now, such methods have not been employed at the continental-scale.

The TherMAP study seeks to bring these modern 3D modelling techniques and apply them to the Australian continent by using the best available geoscientific data to populate the fundamental elements of the heat flow equation (Equation 1). Indeed there are many existing datasets that provide an insight into the range of likely subsurface temperatures across the continent, but which have not been previously utilised at such a scale. With modern computing resources, these various datasets can be brought together into a single, consistent, continental-scale modelling study. Furthermore, the TherMAP study also seeks to begin to answer questions regarding the uncertainties of temperature estimates.

2. METHOD

A Monte Carlo sensitivity analysis process was followed, whereby each of the input variables were allowed to vary freely within their defined uncertainty distributions, and the impact of this on the distribution of output models was examined. This was achieved by first constructing a 3D model of the Australian continent as a Gocad^{TM} voxet, assigning thermal rock properties, and then running a forward model to determine the steady-state thermal equilibrium solution. However, in order to capture uncertainties in both the thermal properties and model structure, 401 individual voxets were constructed and modelled.

The voxets were prepared using the GDA94 / Geoscience Australia Lambert projection (EPSG: 3112), for the rectangular area bound by the coordinates [-2195000, -1120000] and [2100000, -5115000] (approximately [8.1°S, 115.8°E] and [43.6°S, 159.4°E], respectively). The voxets extended from 4,000 mSL to -58,900 mSL. With a voxel count of 400x430x295 (a resolution of approximately 10 km by 10 km by 200 m), the models contained some 50.74 million cells.

The Gocad^{TM} voxets were forward modelled using the Underworld software package (Moresi *et al.*, 2007). Underworld uses a finite-element method to solve the steady-state thermal solution. Each of the models took approximately 11 min to run on 512 CPUs, requiring 1.94 TB of allocated memory, on the NCI's Raijin supercomputer at the ANU.

Reflective, no-flux (Neumann) heat flow boundaries were applied to the sides of the model, while fixed temperature (Dirichlet) boundaries were applied to the top and bottom of the model. The process of defining the various input parameters, and their associated uncertainties, is detailed in the following sections.

2.1 Thermal Conductivity

The bulk thermal conductivity of a sedimentary basin can be estimated by the weighted harmonic mean of all the constituent stratigraphic units. Estimated in this way, it is assumed that all stratigraphic units in all basins are horizontal (i.e. no large scale deformation has occurred; see Beardsmore and Cull, 2001). It is also assumed that all compositional variation occurs as discrete beds (e.g. laminated beds of sandstone and mudstone, rather than sandstone with a clay-rich matrix).

Stratigraphies have been compiled for Australian sedimentary basins. Formations were assigned to each basin based on these stratigraphies, and each formation was assigned a thickness in metres, which was used to determine weightings when calculating mean thermal conductivity values. In most cases the thicknesses assigned were the maximum thickness observed for each formation. It is assumed that all units achieve maximum thickness at the same location in the basin, and that stratigraphic units maintain constant relative thickness in a basin. The pinching out of specific formations is therefore not accounted for. The full stratigraphic sequence of a basin is assumed to be present in all parts of the basin, meaning that changes to local stratigraphy due to folding, faulting or weathering are not accounted for. In many cases basins do not have a single stratigraphy that is representative of the entire basin, or facies changes cause formations to have variable lithology in different areas. In these cases, formations or facies changes were correlated across the basin and an average thermal conductivity for the correlative units was calculated, assuming all correlated units were equally abundant. Unique stratigraphies were only determined for a limited number of sub-basins.

The assigned thermal conductivity values ranged from 1.63 $Wm^{-1}K^{-1}$ to 3.18 $Wm^{-1}K^{-1}$. To date, not all basins have been assigned a bulk thermal conductivity estimate (Figure 1). In areas without specific thermal conductivity information, a default bulk value of 3.0 $Wm^{-1}K^{-1}$ was applied. The default variance for sedimentary basins was set at 0.3 $Wm^{-1}K^{-1}$. Where a bulk thermal conductivity had been estimated for a particular sedimentary basin, this variance was reduced to 0.15 $Wm^{-1}K^{-1}$. The thicknesses of sedimentary basins across the Australian continent have been incorporated into the model voxets using surfaces constructed from the OZ SEEBASE^{TM} report (FROGTECH, 2006).

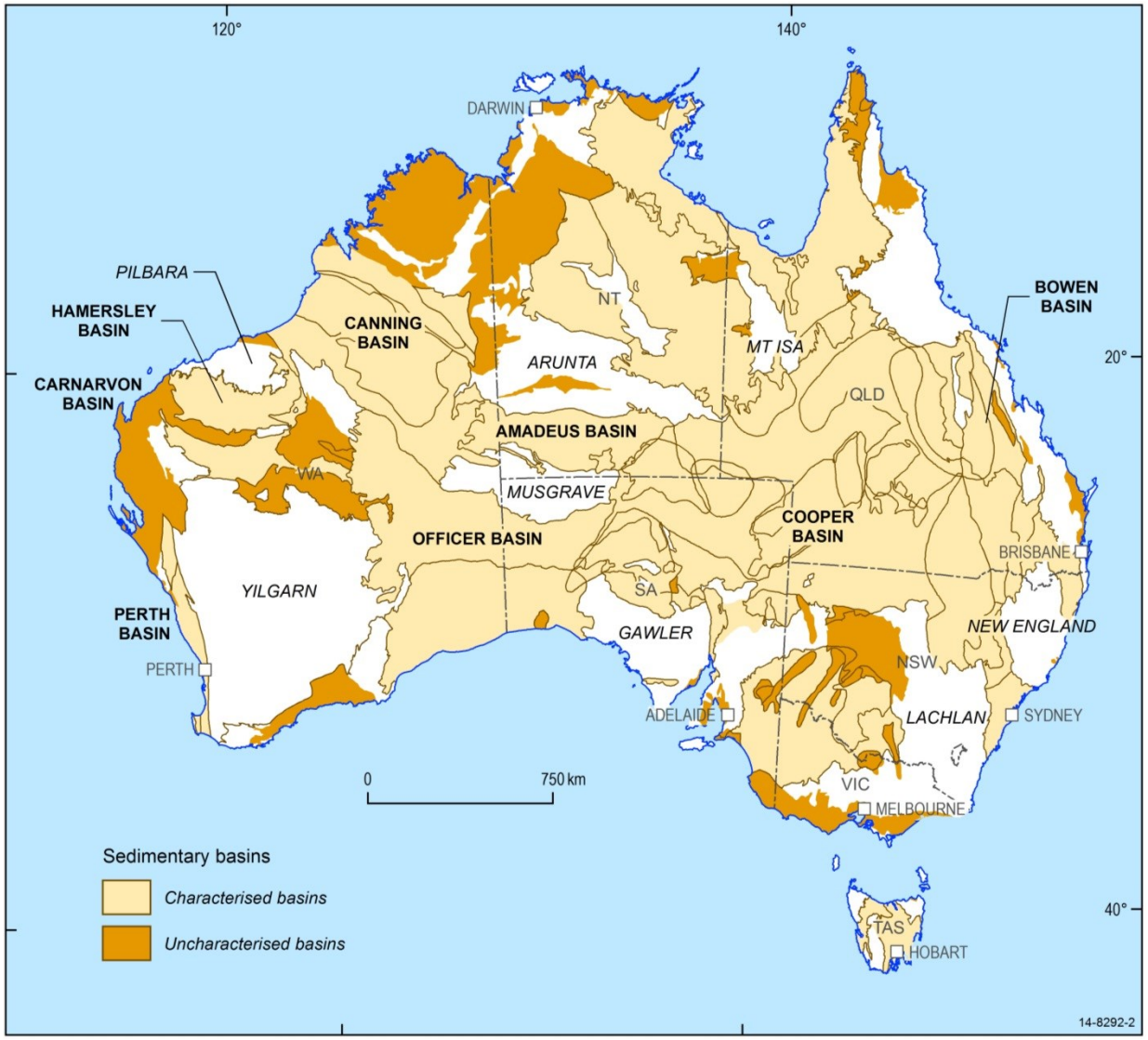

Figure 1: Australian sedimentary basins. Basins where mean thermal conductivity has been estimated for this study are shown in light brown. Basins that have yet to be assessed are shown in dark brown. The names of features that are relevant to the discussion have been provided for context.

Granite bodies were assigned thermal conductivity values according to the properties determined by Meixner *et al.* (2012), who examined the range of granite samples within the Geoscience Australia thermal conductivity database. Their study suggested that Australian granite thermal conductivities fell within the range 2.79 ± 0.38 $Wm^{-1}K^{-1}$.

Meixner *et al.* (2012) adopted thermal conductivity values for the basement beneath the Cooper Basin that were representative of metasedimentary lithologies; this was also adopted for the TherMAP study. While the assumption of a purely metasedimentary basement across the whole continent may not be geologically rigorous, the broad uncertainties over the mean thermal conductivity value conservatively cover the range of values observed in other basement lithologies (Beardsmore and Cull, 2001). Meixner *et al.* (2012) examined the thermal conductivity values for all metasedimentary samples in the Geoscience Australia database, and suggest a value of 3.54 ± 0.89 $Wm^{-1}K^{-1}$.

Rock units above the Moho surface were assigned temperature-dependent thermal conductivity values. The method of temperature dependence adopted in this study was that defined by Sekiguchi (1984), Equation 2, which Beardsmore and Cull (2001) suggest is sufficient in most situations.

$$\lambda = \left(\frac{T_0 T_m}{T_m - T_0}\right)(\lambda_0 - \lambda_m)\left(\frac{1}{T} - \frac{1}{T_m}\right) + \lambda_m \quad (2)$$

Where λ is the thermal conductivity at temperature T, λ_0 is the measured thermal conductivity at temperature T_0 (assumed to be 15°C), and λ_m is the assumed thermal conductivity convergence point at the temperature T_m (set at 1.84 $Wm^{-1}K^{-1}$ and 1200°C, respectively, as per Sekiguchi, 1984).

2.2 Heat Production Rates

A continental-scale assessment of the potential footprint of granitic bodies in the Bouguer gravity dataset has recently been conducted by Petkovic (2014). The identified potential granite locations and their classifications, relative to areas of known granite occurrence, have been incorporated into the present study. Petkovic (2014) broadly separated the potential bodies into three

categories; those that were coincident with known granite occurrences, those that were located only a short distance from them, and those that were located in areas with no known granite occurrence. These categories were used here to define a range of probabilities that an identified rounded gravity low was the footprint of a granite body. Coincident anomalies were assigned a probability of 100%, those that were near known granite occurrences were assigned a probability of 75%, and those that were far were assigned a probability of 50%. With no previous assessment of the reliability of such a study, at the continental-scale, the specific probabilities assigned are arbitrary, but were adopted to induce a degree of variability in the output model.

The potential granite location shapefiles provided a 2D lateral footprint that, after passing the probability test, needed to be used to construct a 3D granite pluton. The thickness of individual granite plutons in this case was estimated using the power-law aspect ratio suggested by Petford *et al.* (2000), Equation 3.

$$D = L^{0.6\pm0.1} \tag{3}$$

Where D is the thickness of the granite pluton in km, and L is the length of the pluton's diameter in km. Heat production rates were then assigned to groups of granite bodies on a province-by-province basis. This was achieved by taking a random sample from the population of granite heat production rates, contained in individual heat-production provinces (provinces modified from Stewart *et al.*, 2013, to remove lateral overlap and to capture observed distribution patterns), based on samples in the OZCHEM database (Champion *et al.*, 2007), as summarised in Table 1.

A thickness of basement with elevated heat production rates was also included in the structural models following the simple approach for crustal heat flow discussed by Roy *et al.* (1968). A constant thickness of 10 km was applied, with heat production rates in this zone set at 4.0 μWm^{-3}, consistent with that for the central Australia heat-flow province (McLaren *et al.*, 2003). A standard deviation of 1.0 μWm^{-3} around this mean heat production estimate was assumed.

For sedimentary rock units, a conservative estimate of 1.0 μWm^{-3} was assigned as a default heat production rate. This was based on the range of values suggested by Meixner *et al.* (2011) for basin units in east-central South Australia.

2.3 Moho Depth and Temperature

For this study, the Moho surface was used to represent the basal boundary condition. The depth of this surface was based on a probabilistic surface reconstruction of the Australian Moho undertaken by Bodin *et al.* (2012). For each model run a Moho surface depth was estimated using a random sample based on the results of Bodin *et al.* (2012). This was achieved by sampling from a lognormal distribution, as defined by Equation 4,

$$X = e^{\mu+\sigma Z} \tag{4}$$

where X is the desired Moho depth raster, Z is the random normal variable (applied as a scalar), and μ and σ are rasters generated from the mean (m) and variance (v) values, from Bodin *et al.* (2012), following Equation 5.

$$\mu = \ln\left(\frac{m^2}{\sqrt{v+m^2}}\right),\ \sigma = \sqrt{\ln\left(1+\frac{v}{m^2}\right)} \tag{5}$$

A single fixed temperature in the range 700 ± 100°C was then assigned to this surface based on the range of values estimated in previous studies (Shan *et al.*, 2011; Abbott *et al.*, 2013), and initial testing on the range of values required to match the observed Australian temperature gradients.

2.4 Surface Temperature

The Underworld software package requires that a single fixed temperature is assigned to the top surface of the voxet. However, through careful manipulation of the thermal conductivity values assigned to the air/water column above the topographic surface of the model, the heat flow equation can be rearranged to approximate the desired temperature change between the top of the voxet and the topographic surface. Thus a spatially-variable, temporally-constant temperature was fixed to the topographic surface.

For this purpose, a raster of the mean annualised surface temperature for the standard 30-year period 1961-1990 (BoM, 2011) was assigned. This raster was then augmented to include modelled sea-floor temperatures (CSIRO, 2009) to help reduce boundary-induced errors. The temperature dependence of the thermal conductivity values assigned to the rock column meant that the surface temperatures could not be exactly matched, as the steady-state thermal conductivity values are not known at the start of the model. However, the error introduced here is expected to be much smaller than the error avoided in attempting to match the surface temperatures in the first instance.

3. RESULTS

The mean and standard deviation of the 401 TherMAP models have been determined for a 4 km deep transect (relative to ground level), and are shown in Figure 2. The results suggest a thermal profile for the Australian continent that is similar to previous continental-scale temperature maps of Australia in some areas, but differing in others.

A large thermal anomaly is immediately apparent from Figure 2a in Western Australia. Elevated temperatures are predicted for the Perth Basin, Carnarvon Basin, Pilbara, Hamersley Basin, Canning Basin and northern Yilgarn Craton areas. Another large thermal anomaly is predicted to occur in north-eastern South Australia, around the area of the Cooper Basin. Almost all other thermal anomalies of note seem to be distributed along much of the Australian coastline, particularly across northern Australia.

Areas of low temperature, at 4 km depth, are notable in central Australia including the Mount Isa and Arunta Orogens, and the Musgrave Province regions. These relatively cold temperatures extend in a south-east trend through the Gawler Craton, Murray

Basin, and into the Lachlan and New England Orogens in south-eastern Australia. In Western Australia, the southern and eastern portions of the Yilgarn Craton are also predicted to exhibit relatively cooler temperatures.

Table 1: Heat production rates for granite samples in the OZCHEM dataset (Champion *et al.*, 2007), grouped by province. *Assigned the same standard deviation as Gascoyne Province due to a lack of samples. **Assigned the same values as Aileron Province due to a lack of samples.

Heat-Production Province	*Mean (μWm^{-3})*	*Standard Deviation (μWm^{-3})*	*Count*
Aileron Province	4.46	3.69	412
Collier Basin	5.62	2.26*	1
Curnamona Province	8.50	14.19	603
Delamerian Orogen	6.29	4.99	78
Gascoyne Province	2.98	2.26	214
Gawler Craton	4.34	3.78	1287
Halls Creek Orogen	2.94	1.86	386
Irindina Province	4.46**	3.69**	0
King Leopold Orogen	3.55	1.17	101
Lachlan Orogen	2.83	1.56	2242
Mossman Orogen	4.48	2.45	1380
Mount Isa Orogen	5.24	3.28	621
Musgrave Province / Paterson Orogen	3.96	3.05	584
New England Orogen	2.32	1.65	2267
North Australian Element	3.23	2.18	932
Pilbara Craton	1.93	1.71	1503
Pine Creek Orogen	5.41	2.44	625
Pinjarra Element	4.50	3.21	8
Tanami Orogen	3.12	2.24	175
Thomson Orogen	2.14	1.35	1135
Warramunga Province / Davenport Province	4.28	2.60	415
Warumpi Province	4.04	3.32	86
Yilgarn Craton, East	2.51	2.49	1952
Yilgarn Craton, North-West	3.22	2.86	34
Yilgarn Craton, South-West	3.32	2.97	67
Yilgarn Craton, West	4.10	2.92	1733

Levels of higher uncertainty (Figure 2b) exhibit, in general, a similar distribution to areas of elevated temperatures. However, the two phenomenon are not entirely coincident. Relatively high uncertainties are reported for the Amadeus and Officer Basins in central Australia, for example; basins that are predicted to exhibit only moderate temperatures at 4 km depth. Furthermore, some areas with predicted high temperatures, such as the Pilbara in Western Australia, have relatively small uncertainties. Overall, the uncertainties produced by the TherMAP models fall between 15-30°C, except for a number of thermal anomalies in the Curnamona Province in South Australia, where the standard deviation reaches 207°C.

4. DISCUSSION

TherMAP has brought together a range of datasets to populate the heat flow equation (Equation 1). This has built a stronger geoscientific basis by which to estimate temperatures in areas that are distant from direct bottom-hole temperature observations. Furthermore, by incorporating these datasets into a stochastic framework, TherMAP has also been able, for the first time, to begin to answer questions regarding the relative uncertainties of different temperature estimates at the continental scale. All of this has been achieved without direct use of the OzTemp bottom-hole temperature dataset (Holgate and Gerner, 2010), which allows this information to be used for validation purposes and to help refine the modelling assumptions.

Comparisons can first be made between the TherMAP results and the OzTemp map of interpreted temperatures at 5 km (Gerner and Holgate, 2010; Figure 3). While these images represent temperature estimates at different depths, some comments can be made regarding the differing trends between the two studies. Promisingly, TherMAP has reproduced some of the features that have been observed through drilling and are highlighted in the OzTemp map; in particular, around the Cooper and Bowen Basins in central Australia and eastern Queensland, respectively. Indeed, some models have been able to accurately estimate the observed bottom-hole temperatures in the either of basins within approximately ±10°C (for example, Figure 4).

The OzTemp map (Figure 3) also highlights that relatively high bottom-hole temperatures have been observed in patchy distributions in the Perth, Carnarvon, and Canning Basins. Large areas of northern Northern Territory and northern Queensland are also shown to have observations of relatively high bottom-hole temperatures. In these areas, the TherMAP modelling also suggests higher temperatures (~100°C at 4 km depth), though the nature of these anomalies is now more reflective of the geological settings in which they are found.

There are, however, some areas of substantial difference between the two studies. Most notable is a large area of Western Australia covering the northern Yilgarn, Hamersley Basin and the Pilbara. The OzTemp map predicts temperatures in this area that are among the coldest across the continent (< 85°C at 5 km depth), albeit with very few data points. In TherMAP, these areas are now estimated to be amongst the warmest (~110-120°C at 4 km depth; Figure 2a).

Validation of the TherMAP subsurface temperature estimates was also attempted through direct comparison with the exact bottom-hole temperatures recorded in the OzTemp dataset (Holgate and Gerner, 2010). The regular gridding of the TherMAP voxets allowed an easy comparison to be made to the XYZ OzTemp data (where the Z-axis was calculated as depth relative to ground level), through tri-linear regression of the estimated temperatures at the eight nearest voxet nodes.

A root mean square error value was determined for the comparison of each TherMAP model with the OzTemp bottom-hole temperature dataset. Across the 401 TherMAP models, this error metric averaged 56.9 ± 6.5°C. An explanation for this large error value can be given from inspection of the errors reported for individual runs, which show similar trends across many models. An example is shown from model run '*TherMAP_2014-04-22_12-51*' (Figure 4) highlighting the characteristic error distributions. Notably, three distinct trends can be seen that correlate with the three major groupings of OzTemp data points around the North-West Shelf, the Cooper Basin and the Bowen Basin. What is also highlighted is that, under the inputs and assumptions of the current modelling process (specifically the largely unconstrained upper-crustal heat production and the fixed Moho temperature), the TherMAP models appear unable to replicate the measured conditions across these different locations within a single model and predict, in general, cooler temperatures than are observed.

Mean error statistics, on a point-by-point basis, have not yet been calculated for the comparison to the OzTemp dataset across the ensemble of TherMAP models. However, initial analysis suggests that, when plotted spatially, these errors represent broad trends that vary smoothly across much of the continent. Given this, it may be possible to determine a corrective factor that could be applied to the mean temperature estimate to compensate for the limiting Moho assumptions, and better approximate the subsurface conditions.

Another factor that may be adding to the observed errors is the assumption of a purely conductive system. In the current TherMAP method, an empirical temperature dependence is applied to rock thermal conductivity values (Equation 2; Sekiguchi, 1984), which has the effect of substantially lowering these values with increases in temperature. However, at temperatures higher than 300°C the radiative component of heat transfer begins to play an increasingly significant role (Beardsmore and Cull, 2001), raising the effective thermal conductivity. In TherMAP, the temperature at the Moho is set substantially higher than 300°C (at 700 ± 100°C), and as such the applied thermal conductivity value may be lower than should be required.

The hypothesis that a lack of radiative heat transfer is one of the key contributors to the observed errors is supported from the nature and distribution of uncertainties reported for the model (Figure 2). From visual inspection there appears to be a strong link between the levels of uncertainty and sedimentary thickness (FROGTECH, 2006). A reason for this apparent correlation would be due to the high levels of uncertainty in the predicted Moho depth (Bodin *et al.*, 2012) which, with a fixed Moho temperature, would cause some models to be run with an extremely high heat flow. The extra thermal resistance of sedimentary basins would amplify the temperatures in these models and could potentially cause the observed higher uncertainties. It may be that increasingly-high Moho temperatures are required in TherMAP to compensate for the increasingly-large error associated with ignoring radiative heat transfer.

The current magnitude of the validation errors suggests that there is much work that can be done to further constrain the modelling inputs and assumptions. It is therefore suggested that future developments with TherMAP focus on three aspects:

- Spatially variable basal boundary conditions. Previous studies have predicted that the Moho can vary in temperature from location to location (for example; Shan *et al.*, 2011). Allowing this temperature to vary (or moving to a variable heat flow boundary condition, see below) may allow the conditions to be better predicted across the continent and hence enhance the accuracy of the temperature predictions achieved.

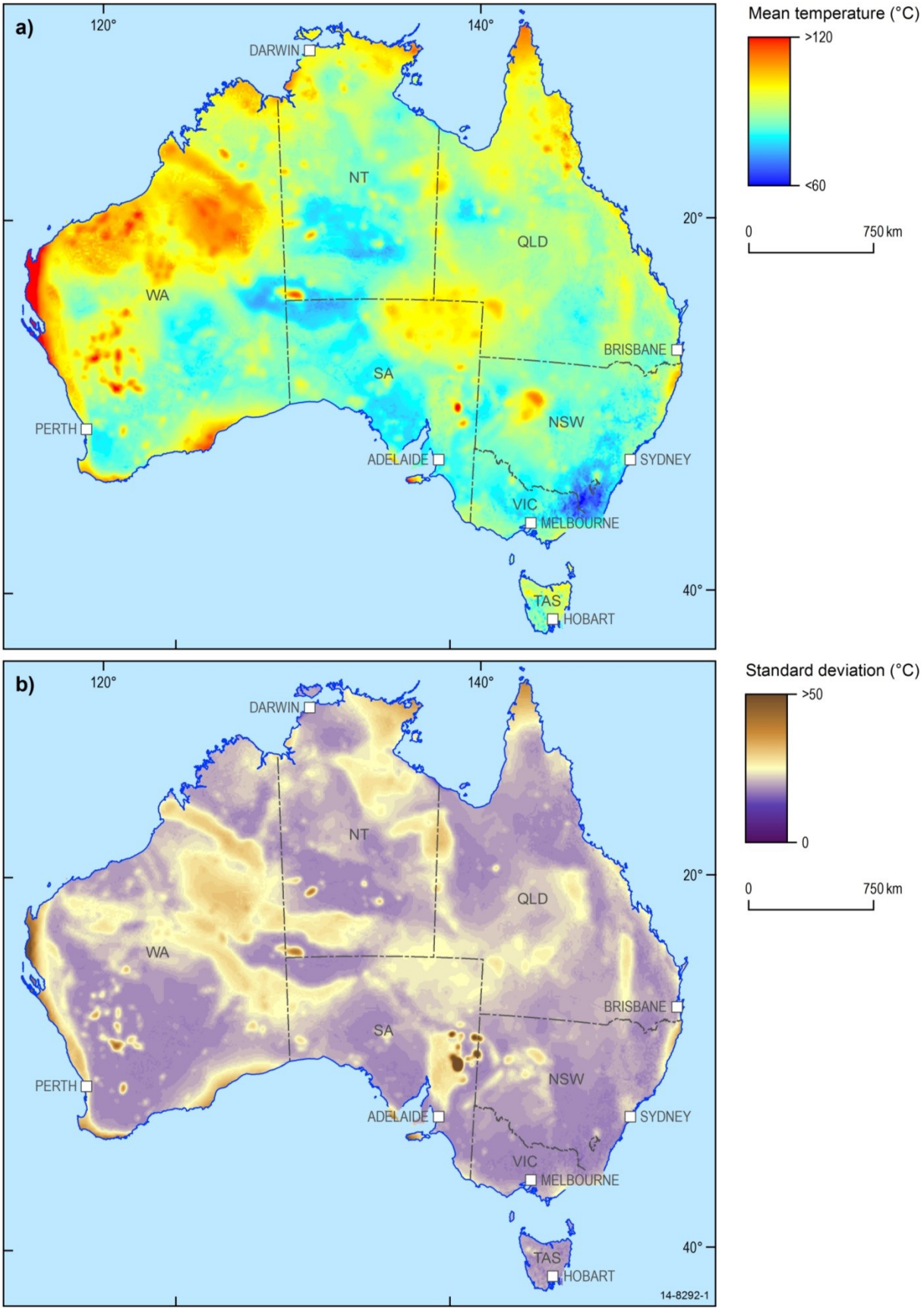

Figure 2: Results of the 401 TherMAP models at 4 km depth relative to ground level. A) The mean estimated subsurface temperature from the ensemble of models. B) The standard deviation from the ensemble of models.

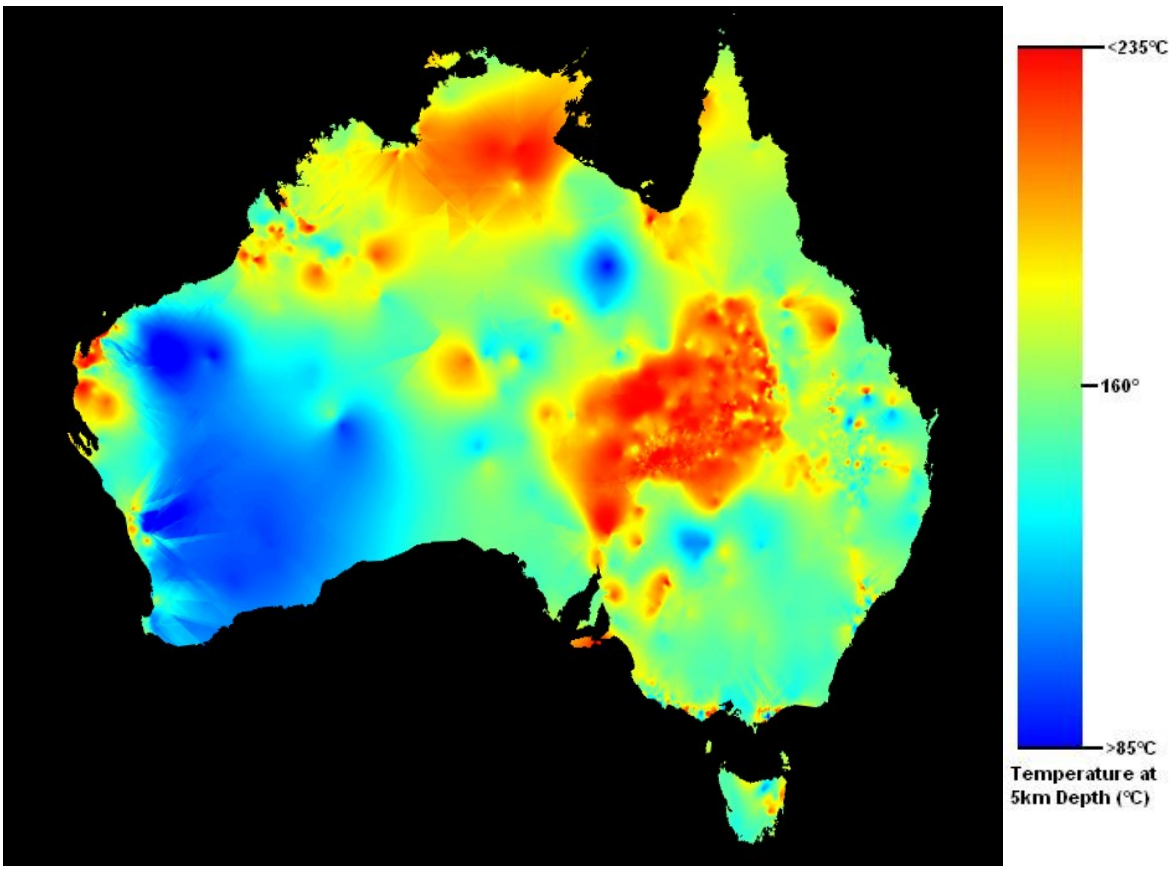

Figure 3: '*OzTemp – Interpreted Temperature at 5km Depth Image*' (Gerner and Holgate, 2010).

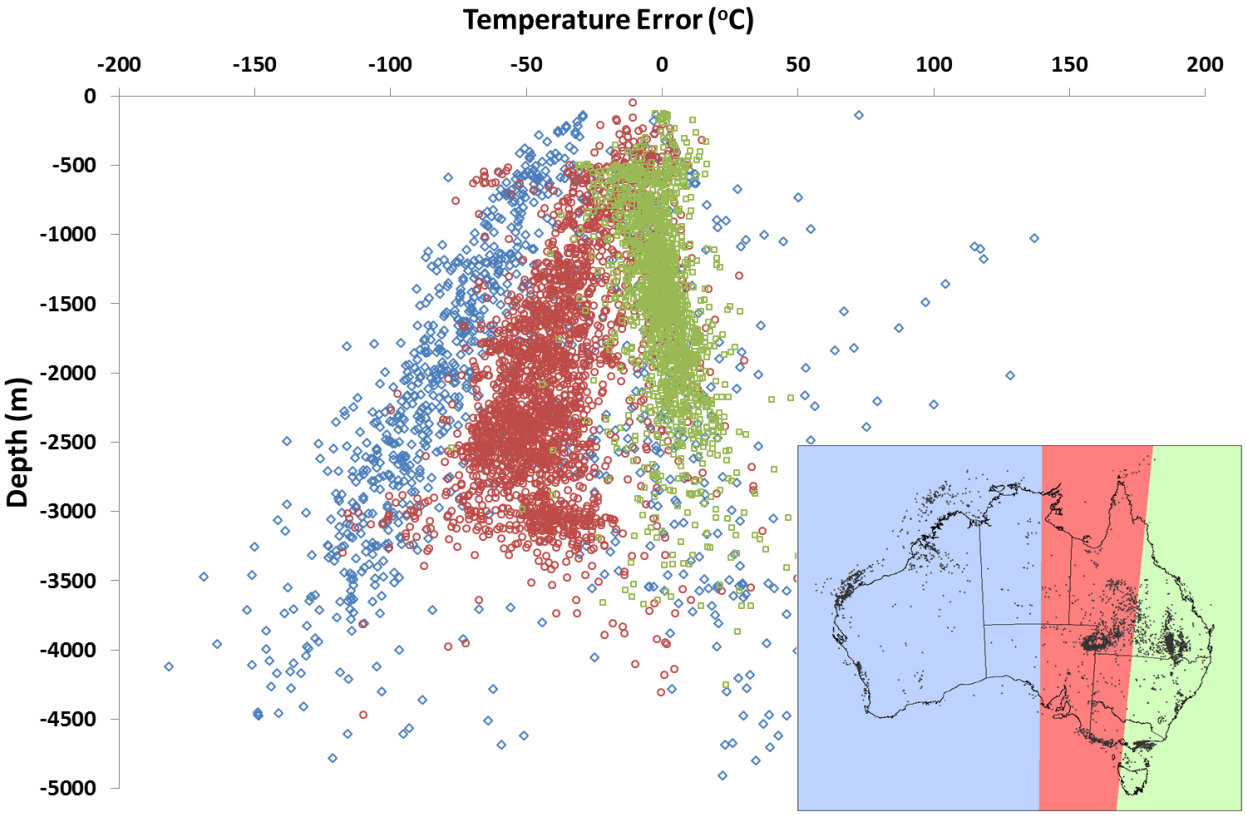

Figure 4: Temperature prediction errors for model TherMAP_2014-04-22_12-51; negative values indicate that the estimated temperature is cooler than the observed temperature. The data have been divided into three groupings based on longitude; blue diamonds are located west of 135°E, green squares are located east of 145°E, and red circles are located between 135°E and 145°E. These groupings and the locations of the data points are shown in the inset.

- Use of a basal heat flow boundary condition. An improvement for future studies could be to set the basal boundary condition using a fixed (though spatially variable) heat flow. Following the methods of previous studies, including Roy *et al.* (1968) and McLaren *et al.* (2003), it may be possible to extract mantle heat flow rates and upper crustal heat production from determinations of surface heat flow. This would provide a geoscientific basis for the basal boundary condition, and may go some way to determining some reasonable bounds for the Australian Moho temperature and / or may further constrain the uncertainties surrounding the Moho depth.
- A greater appreciation of the interplay between effective thermal conductivity and temperature. This is especially important given the increasing role that radiative heat transfer plays at high temperatures. If a better understanding can be achieved of the effective thermal conductivity of rocks at high temperatures, it seems likely that reasonable model results could be achieved at lower Moho temperatures. This may, in turn, reduce the magnitude of uncertainties across the ensemble of TherMAP models.

An important outcome of the TherMAP study is that the range of values that have gone into producing a particular temperature estimate at any location are defined and can be interrogated. Previously, validation of the predicted temperatures could only really be achieved where there were a large number of congruous observations predicting similar temperature gradients. Outside of these areas, there was very little geoscientific basis behind the estimated temperatures. TherMAP, however, has the ability to shift the focus of subsequent exploration steps towards elements that are relatively cheap and quick to evaluate, by focusing on how well the input data approximates reality. For example, choosing whether to undertake a seismic survey to test the presence and size of predicted granite bodies, or undertaking geochemical analysis to confirm localised heat production rates. Such initial steps can substantially reduce the risks involved in evaluating prospective plays prior to expensive drilling.

5. CONCLUSIONS

There are greater amounts of geoscientific data available in Australia by which to estimate subsurface temperatures than have previously been utilised. The utility of these datasets has been unlocked by adopting a geothermal systems perspective for thermal modelling together with modern 3D thermal modelling techniques. The results of this process have reproduced the large observed thermal anomaly in the Cooper Basin area of central Australia, and have also raised questions about estimated high temperatures over large areas of northern Western Australia. Indeed, while the specific subsurface temperature estimates produced by TherMAP remain cooler than observed conditions, the distribution of thermal anomalies suggests that numerous areas across the country may reach temperatures that are required for electricity production (> 150°C) at depths of 4 km. At this stage, the uncertainties around many of the estimated thermal anomalies remain high (±30°C) but, by basing these estimates on specific input values, there are relatively easy steps that can be taken to further validate the results in areas of interest.

ACKNOWLEDGEMENTS

The authors would like to thank Bridget Ayling and David Lescinsky for taking the time to critically review this work. The authors would also like to thank David Lescinsky and Chris Harris-Pascal for assistance in preparing some of the input datasets. This research was undertaken on the NCI National Facility in Canberra, Australia, which is supported by the Australian Government.

This paper is published with the permission of the CEO, Geoscience Australia.

REFERENCES

Abbott, D.H., Mooney, W.D. and VanTongeren, J.A.: The Character of the Moho and Lower Crust Within Archean Cratons and the Tectonic Implications. *Tectonophysics*, **609**, (2013), 690-705.

Beardsmore, G. and Cull, J.: *Crustal Heat Flow: a Guide to Measurement and Modelling*. Cambridge University Press, United Kingdom, (2001).

Beardsmore, G., Rybach, L., Blackwell, D. and Baron, C.: A Protocol for Estimating and Mapping Global EGS Potential. *Proceedings of the Australian Geothermal Energy Conference 2010*, 16-19 November, Adelaide, Australia (2010).

Bodin, T., Salmon, M., Kennett, B.L.N. and Sambridge, M.: Probabilistic surface reconstruction from multiple data sets: An example for the Australian Moho. *Journal of Geophysical Research*, **117**, (2012), B10307, doi: 10.1029/2012JB009547.

BoM (Bureau of Meteorology): *Average annual & monthly maximum, minimum, & mean temperature*. [Online], (2011), available: http://www.bom.gov.au/jsp/ncc/climate_averages/temperature/index.jsp?maptype=6&period=an

Champion, D.C., Budd, A.R., Hazell, M.S and Sedgmen, A.: *OZCHEM National Whole Rock Geochemistry dataset*. [Online], (2007), available: http://www.ga.gov.au/metadata-gateway/metadata/record/gcat_a05f7892-d0ec-7506-e044-00144fdd4fa6/OZCHEM+National+Whole+Rock+Geochemistry+Dataset

Chopra, P. and Holgate, F.L. 2005. A GIS Analysis of Temperature in the Australian Crust. *Proceedings of the World Geothermal Congress 2005*, 24-29 April, Antalya, Turkey, (2005).

Cooper, G.T. and Beardsmore, G.R. 2010. Engineered Geothermal Systems in the Australian Context – Resource Definition in Conductive Thermal Settings. *Proceedings of the World Geothermal Congress 2010*, 25-29 April, Bali, Indonesia, (2010).

CSIRO: *CSIRO Atlas of Regional Seas*. [Online], (2009), available: http://www.cmar.csiro.au/cars

Danis, C.R. and O'Neill, C.: The 3D Basement and Thermal Structure of the Gunnedah Basin. *Proceedings of the Australian Geothermal Energy Conference 2009*, 11-13 November, Brisbane, Australia, (2009).

Felix, M., Förster, A., Förster, H.J., Konietzky, H. and Wagner, S.: Exploration Strategy for a Deep EGS Development in Crystalline Rocks (Germany). *GRC Transactions*, **34**, (2010), 335-338.

FROGTECH: *OZ SEEBASE™ Proterozoic Basins Study*, Report to Geoscience Australia by FROGTECH Pty Ltd. Canberra, Australia, (2006).

Gerner, E.J., and Holgate, F.L.: *OZTemp – Interpreted Temperature at 5 km Depth Image*, [Online], (2010), available: www.ga.gov.au.

Gerner, E.J., Holgate, F.L. and Budd, A.R.: OZTEMP: An Updated Map and Database for Predicting Temperature at Five Kilometres Depth in Australia. *GRC Transactions*, **34**, (2010), 345-346.

Holgate, F.L. and Gerner, E.J.: *OZTemp Well Temperature Data*. [Online], (2010), available: www.ga.gov.au.

McLaren, S., Sandiford, M., Hand, M., Neumann, N., Wyborn, L. and Bastrakova, L.: Chapter 12 – The hot southern continent: heat flow and heat production in Australian Proterozoic terranes. *Geological Society of Australia Special Publication*, **22**, (2003), 151-161.

Meixner, A.J., Kirkby, A., Champion, D.C., Weber, R., Connolly, D. and Gerner, E.: *Geothermal systems. An assessment of the uranium and geothermal prospectivity of east-central South Australia*. Geoscience Australia Record **2011/34**, Canberra, Australia, (2011), 166-207.

Meixner, A.J., Kirkby, A.L., Lescinsky, D.T. and Horspool, N.: *The Cooper Basin 3D Map Version 2: Thermal Modelling and Temperature Uncertainty*. Geoscience Australia Record **2012/60**, Canberra, Australia, (2012).

MIT (Massachusetts Institute of Technology): *The Future of Geothermal Energy: Impact of Enhanced Geothermal Systems (EGS) on the United States in the 21st Century*. MIT Press, Cambridge, USA, (2006), Chapter 2.

Moresi, L., Quenette, S., Lemiale, V., Meriaux, C., Appelbe, C., and Mühlhaus, H.B.: Computational approaches to studying non-linear dynamics of the crust and mantle. *Physics of the Earth and Planetary Interiors*, **163**, (2007), 69-82, doi: 10.1016/j.pepi.2007.06.009.

Petford, N., Cruden, A.R., McCaffrey, K.J.W. and Vigneresse, J.L.: Granite magma formation, transport and emplacement in the Earth's crust. *Nature*, **408**, (2000), 669-673.

Petkovic, P.: *Gravity and granites: Technical notes on mapping relationship between known granites and gravity*. Geoscience Australia Record **2014/12**, Canberra, Australia, (2014), 1-33.

Roy, R.F., Blackwell, D.D. and Birch, F.: Heat Generation of Plutonic Rocks and Continental Heat Flow Provinces. *Earth and Planetary Science Letters*, **5**, (1968), 1-12.

Sass, J.H. and Lachenbruch, A.H.: Thermal Regime of the Australian Continental Crust. In: *The Earth: It's Origin, Structure and Evolution*. McElhinny, M.W. (Ed.), Academic Press, London, United Kingdom, (1979).

Sekiguchi, K.: A method for determining terrestrial heat flow in oil basinal areas. *Tectonophysics*, **103**, (1984), 67-79.

Shan, J-N., Zhang, G-C., Tang, X-Y., Wu, J-F., Zhao, C-Y., Song, Y. and Hu, S-B.: Thermal Structure and Moho Temperature of the Qiongdongnan Basin, Northern Margin of the South China Sea. *Chinese Journal of Geophysics*, **54(4)**, (2011), 516-525.

Somerville, M., Wyborn, D., Chopra, P., Rahman, S., Estrella, D. and Van der Meulen, T.: *Hot Dry Rock Feasibility Study*. Energy Research and Development Corporation, Australia, (1994).

Stewart, A.J., Raymond, O.L., Totterdell, J.M., Zhang, W. and Gallagher, R.: *Australian Geological Provinces, 2013.01 Edition*. [Online], (2013), available: http://www.ga.gov.au/metadata-gateway/metadata/record/gcat_c3fac1d5-48c1-624e-e044-00144fdd4fa6/Australian+Geological+Provinces%2C+2013.01+edition